ISSN 1029-9599, Physical Mesomechanics, 2020, Vol. 23, No. 4, pp. 324–331. © Pleiades Publishing, Ltd., 2020.
Russian Text © The Author(s), 2019, published in Fizicheskaya Mezomekhanika, 2019, Vol. 22, No. 5, pp. 54–61.

Study on the Size Dependence of Calibration Parameters of the New Local Approach Model for Cleavage Fracture

A. R. Shen[1], P. C. Li[1]*, Z. S. Yu[2], G. A. Qian[3], F. Berto[4], and W. Wu[5]*****

[1] *School of Mechanical and Automotive Engineering, Shanghai University of Engineering Science, Shanghai, 201620 China*
[2] *School of Materials Engineering, Shanghai University of Engineering Science, Shanghai, 201620 China*
[3] *State Key Laboratory for Nonlinear Mechanics, Institute of Mechanics, Chinese Academy of Sciences, Beijing, 100190 China*
[4] *Department of Mechanical and Industrial Engineering, Norwegian University of Science and Technology, Trondheim, 7491 Norway*
[5] *Institute of Advanced Structure Technology, Beijing Institute of Technology, Beijing, 100081 China*
* *e-mail: wiselee@sues.edu.cn*
** *e-mail: qianguian@imech.ac.cn*
*** *e-mail: wuwenwang@bit.edu.cn*

Received July 22, 2019, revised July 22, 2019, accepted July 31, 2019

Abstract—This paper investigates whether the Weibull parameters of the new local approach model for cleavage fractures are affected by the geometric size of the specimen. Based on the fracture test data of A508-C steel, low temperature round notched bar tensile specimens of A508-C steel with two different notch sizes are numerically simulated by using finite element analysis software ABAQUS, and the stress distributions are obtained. The Weibull parameters of two notched bars are calibrated by linear regression method. The results show that the Weibull parameters of the specimens with different notch sizes are different. This suggests that the calibration parameters are dependent on the notch size.

Keywords: cleavage fracture, new local approach model, Weibull parameters, notch size

DOI: 10.1134/S1029959920040062

NOMENCLATURE

dV—differential volume, mm^3;
E—Young's modulus, MPa;
F—external load, kN;
i—the serial number of the specimen;
m—Weibull modulus;
N—total number of the specimen;
P—probability of cleavage fracture;
$P(i)$—prescribed probability for the ith specimen;
r—notch radius, mm;
V_0—mean volume occupied by each microcrack in a solid, mm^3;
V_{pl}—plastic volume, mm^3;
ν—Poisson's ratio;
σ_0—Weibull scale parameter, MPa;
σ_1—maximum tensile principal stress, MPa;
$\sigma_{1,0}$—value of σ_1 at initial yield of a differential volume element dV, MPa;
σ_{vM}—von Mises stress, MPa;
σ_W—Weibull stress, MPa;
$\sigma_{W,new}$—newly defined Weibull stress, MPa;
σ_{ys}—yield stress, MPa.

1. INTRODUCTION

Cleavage fracture [1] is a kind of brittle fracture, which is the most dangerous form of fracture and often leads to disastrous failure in engineering applications [2], such as the brittle fracture of reactor pressure vessels [3]. Therefore, cleavage fracture has been the focus of research from many researchers in recent years [e.g., 4–7]. Cleavage fracture consists of three nonstop successive stages: nucleation of a crack in a second-phase particle; the second phase particle-sized crack propagates across the particle and grain boundary; grain-sized crack extends through grain boundary into contiguous grains [8, 9]. In order to properly assess the fracture of a structure, local approach models [10] of fracture have been developed in the past 30 years. There are four commonly used local approach models [11]. Among them, Beremin model

[12] is the only one related to the cleavage fracture. The Beremin model is a two-parameter Weibull distribution model based on the weakest link theory. It was first proposed by the Beremin group to describe the cleavage fracture probability [13, 14]:

$$P = 1 - \exp\left[-\left(\frac{\sigma_W}{\sigma_0}\right)^m\right], \quad (1)$$

$$\sigma_W = \left(\int_{V_{pl}} \sigma_1^m \frac{dV}{V_0}\right)^{1/m}, \quad (2)$$

where P is the probability of cleavage fracture, σ_W denotes the Weibull stress, σ_0 is the Weibull scale parameter, which represents the critical cleavage fracture stress in the Beremin model, m is the Weibull modulus representing the microscopic defect uniformity that may cause cleavage fracture, V_{pl} denotes the integral volume as well as the plastic zone volume, σ_1 is the maximum principal stress of each plastic zone volume element, V_0 is a reference volume, which represents the mean volume occupied by each microcrack in a solid, dV represents the differential volume.

Before a proper application of the Beremin model, two Weibull parameters of the model (i.e., m and σ_0 have to be calibrated according to the existing fracture data [15]. Minami [16] and the European Structural Integrity Society (ESIS) [17] proposed a calibration procedure. The Weibull parameters m and σ_0 have been considered to be inherent parameters of the material completely independent from the external conditions. Accordingly, they have not been considered to be affected by temperatures and loading conditions, as well as the geometric size of the specimens. But more recent studies have contradicted this simplistic hypothesis. For example, Akbarzadeh and Hadidimoud [18] have investigated the dependence of Weibull parameters on geometric size by using round notched bar tensile specimens on the basis of a series of fracture experiments. They have tested eight groups of specimens having a net cross-section diameters of 10 and 15 mm, and notched radius of 5, 4, 2, and 0.2 mm for each group, respectively. The have measured value of m ranging from 6 to 117. The fluctuation of m has been found so wide that it has been clearly shown how much inappropriate would have been to select a fixed value of m independent of the specimen shape and size. Cao et al. [19] have studied the temperature dependence of Beremin model parameters in ductile-to-brittle transition region with the master curve method. The experimental data of 16MnR steel have shown that in the lower transition region, as the temperature increases, the Weibull modulus m decreases. In the lower-to-mid transition region, m remains constant. Within the range of temperature under investigation in [19], the Weibull scale parameter σ_0 increases with the increase of the temperature.

In order to tackle the problem that the Beremin parameters vary with temperatures and geometric constraints, several researchers have revised the initial model originally proposed by Beremin [e.g., 20–22]. However, most of these methods are empirical modifications and lack of a relevant theoretical basis. Based on the Beremin model, Lei [23] has proposed a new cumulative failure probability model of local approach, which is based on the assumption of weakest link and requires that the plastic yield is the prerequisite for the occurrence of cleavage fracture:

$$P = 1 - \exp\left[-\left(\frac{\sigma_{W,new}}{\sigma_0}\right)^m\right], \quad (3)$$

$$\sigma_{W,new} = \left[\int_{V_{pl}} (\sigma_1 - \sigma_{1,0})^m \frac{dV}{V_0}\right]^{1/m}, \quad (4)$$

where $\sigma_{W,new}$ is the newly defined Weibull stress. Compared to the Beremin model, the new model introduces the maximum principal stress at the initial yield $\sigma_{1,0}$ of the differential volume unit dV. As mentioned in Lei [24], in the Beremin model, the Weibull stress σ_W is calculated by the instantaneous maximum principal stress σ_1 in each volume element. When a specific volume element dV just reaches the initial plastic yield, there is $\sigma_1 = \sigma_{1,0}$, according to Eq. (1), the minimum probability for the nonoccurrence of fracture is always different from zero. This is a nonsense from the physical point of view and violates the hypothesis that the plastic yielding is a necessary but insufficient condition for cleavage fracture. This is also the fundamental reason for the change of m and σ_0 with temperatures and geometric sizes during the calibration process. Conversely, in the new model, the stress increment $(\sigma_1 - \sigma_{1,0})$ after initial plastic yield of each element is introduced to calculate the failure probability, which strictly follows the physical mechanism of plastic yield and takes plastic yield as the prerequisite for cleavage fracture. Therefore, Eq. (3) is considered to be able to overcome the ambiguity of the calibration of Weibull parameters. In addition, Qian et al. [25] have recently explained that the new

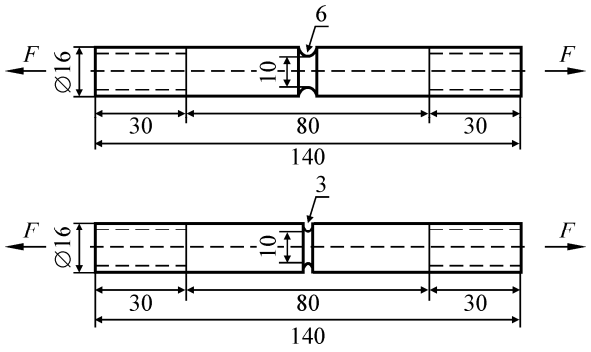

Fig. 1. Round notched bar tensile specimens with notch radius of 6 and 3 mm. All sizes are in mm.

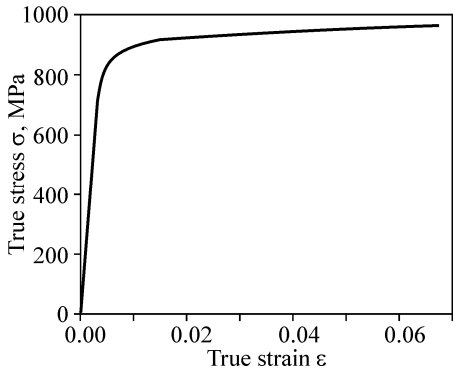

Fig. 2. True stress–strain curve of A508-C steel at –196°C.

model can overcome the ambiguity of the parameters calibration of the Beremin model in details from the perspective of physics and mechanics. Besides, the temperature independence of parameters calibration of the new model has been verified by using circumferentially notched round tensile specimens, but the effect on the geometric size has not been studied in depth. Therefore, the objective of this work is to investigate whether the calibration of Weibull parameters (m and σ_0) is affected by the geometric size in the new local approach model by using two groups of fracture specimens with different notch radii.

2. EXPERIMENTAL DATA

In order to study the effect of geometric size on the two Weibull parameters, two kinds of round notched bar tensile specimens with different notch sizes are used in this work. The notch radii are 3 and 6 mm, respectively. The specimens under loading are shown in Fig. 1. The experimental material is A508-C steel and the experimental data are available from Ref. [26]. Table 1 shows the chemical composition of A508-C steel. The yield stress and Young's modulus of A508-C steel at –196°C are $\sigma_{ys} = 898$ MPa and $E = 2.14 \times 10^5$ MPa. Poisson's ratio $\nu = 0.3$. Figure 2 represents the true stress–strain curve of A508-C steel at –196°C. In [26], Hui and Li made low-temperature tensile tests on the rods with notch radius of 3 and 6 mm, respectively. Among them, 13 groups of specimens with notch radius of 3 mm and 5 groups of specimens with notch radius of 6 mm were tested at the low temperature. The tensile fracture loads of two kinds of specimens are summarized in Table 2.

3. FINITE ELEMENT ANALYSIS AND WEIBULL PARAMETERS CALIBRATION

3.1. Finite Element Analysis and Calibration Method

In this work, the 3D elastic-plastic finite element analysis is used to numerically analyze the specimens. Considering the geometric symmetry and the loading symmetry of the specimens, we only select 1/8 of the structure for modeling so as to reduce the computational time. The element employed in this work is C3D20R. It is worth noting that the grids in the notch region need to be refined. The number of elements are 546624 for notched specimen with r = 6 mm and 510692 for notched specimen with r = 3 mm, respectively. The calibration procedure developed by Qian et al. [25] for the new local approach model is adopted in this work. In the procedure, the process of finite element analysis includes two steps. In the first step, the distribution of the maximum principal stress σ_1 of each volume element is obtained by using the true elastic-plastic hardening constitutive law for the material. As stated by Qian et al. [27], due to the uneven stress distribution of the notch, plastic yield may occur at different time for each volume element, and the maximum principal stress of each unit may be different at the initial yield. In order to obtain the maximum principal stress $\sigma_{1,0}$ of differential volume element dV introduced in Eq. (4), we assume the material as a perfect elastic-plastic material in the second step of the finite element simulation. Then the maximum principal stress of each element in the plastic zone is taken as $\sigma_{1,0}$. The distributions of the maximum principal stress of the two specimens at –196°C are shown in Figs. 3 and 4.

Table 1. Chemical composition of A508-C steel (wt %)

C	Si	Mn	P	S	Ni	Gr	Mo	V	Cu	Co
0.20	0.25	1.22	0.01	0.007	0.72	0.09	0.52	0.003	0.066	0.014

Table 2. Tensile fracture loads of specimens with notch radius of 3 and 6 mm at –196°C

Fracture specimens	Fracture loads of specimens, kN	
	r = 3 mm	r = 6 mm
1	95.79	92.08
2	94.04	92.11
3	96.57	92.50
4	97.73	92.51
5	98.55	93.32
6	99.21	/
7	99.38	/
8	99.40	/
9	99.53	/
10	99.54	/
11	99.55	/
12	99.65	/
13	100.58	/

According to the result file of ABAQUS, we can obtain the number, volume, and corresponding values of σ_1 and $\sigma_{1,0}$ of each plastic zone element. The volume of the plastic zone here is defined as the volume of the unit of $\sigma_1 \geq 1.0\sigma_{ys}$ [28].

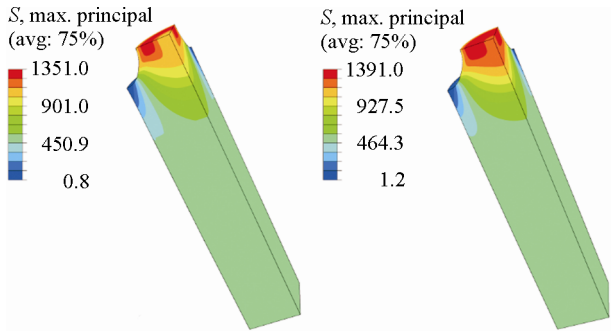

Fig. 3. Distribution of σ_1 in the notched specimen with r = 3 mm at –196°C. The external load is 95.79 (a) and 100.58 kN (b) (color online).

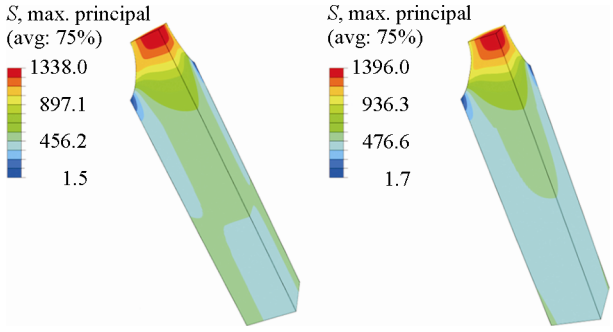

Fig. 4. Distribution of σ_1 in the notched specimen with r = 6 mm at –196°C. The external load is 92.08 (a) and 93.32 kN (b) (color online).

Then the above results can be substituted into Eq. (4) to calculate the Weibull stress. Here we take $V_0 = 0.001$ mm^3. Since the value of m in Eq. (4) is unknown, we assume that the initial value of m is 10, and then the linear regression method is used to calibrate the two Weibull parameters. Equation (3) can be rewritten as follows [29]:

$$\ln\ln(1/(1-P)) = m\ln\sigma_{W,new} - m\ln\sigma_0. \qquad (5)$$

In the linear regression method, the cumulative failure probability P is calculated according to the fracture loads of the specimens in ascending order. Assuming that there are N specimens, the fracture probability of the ith specimen is calculated by the formula $P(i) = (i-0.5)/N$. The value of m can be calibrated from Eq. (5), and the value of σ_0 can be calculated via the intercept term, where the intercept term is $-m\ln\sigma_0$.

3.2. Results of Weibull Parameter Calibration

Figure 5 illustrates the calibration results of Weibull modulus m for round notched bar tensile specimens with notch radius of 3 and 6 mm. The calibration results of Weibull parameters for two specimens at –196°C are provided in Table 3. Table 3 reveals that both the values of m and σ_0 of the two kinds of specimens are significantly different.

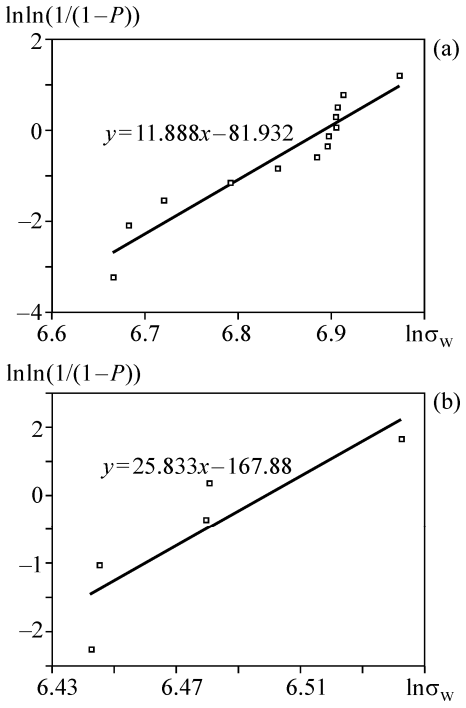

Fig. 5. Calibration result of m of round notched bar tensile specimens with r = 3 (a) and 6 mm (b).

Table 3. Calibration results of Weibull parameters for specimens with different notch radii

r, mm	m	σ_0, MPa
3	11.888	984.360
6	25.833	664.255

That is to say, when the notch sizes of the specimens are different at a given temperature, the corresponding Weibull parameters make a difference.

4. ANALYSIS AND DISCUSSION

As stated above, we can see that the calibration results of the new model parameters are influenced by the geometric size. Specimens with different notch sizes correspond to different Weibull parameters. Akbarzadeh and Hadidimoud [18] have studied the dependence of Weibull parameters on geometry in the Beremin model. They have pointed out that the dependence of parameters on geometric size can be attributed to the stress concentration, but they did not explain it in details. In view of this, we investigate the stress concentration of two kinds of round notched bar tensile specimens with different notch radii. By looking up the practical stress concentration manual [30], we know that the stress concentration factor of round notched bar tensile specimen with notch radius of 3 mm is about 1.57, while it is about 1.32 in the case of notch radius of 6 mm. Obviously, when the notch radius is different, the stress concentration factor of the specimen is different. In addition, we examine the influence of notch depth on the maximum principal stress of the two types of specimens. The curves of the maximum principal stress with the distance from the notch root under different loads are displayed in Fig. 6.

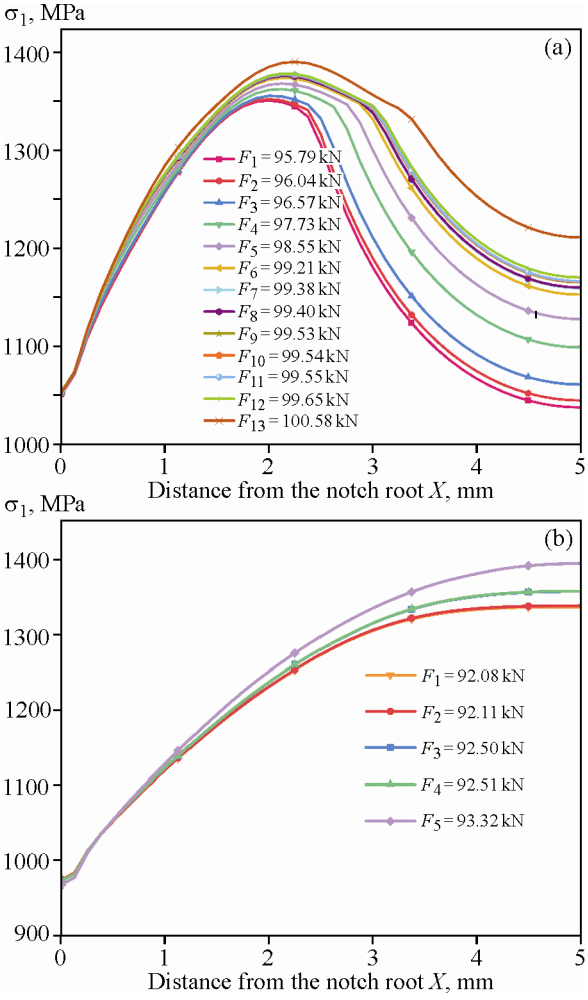

Fig. 6. Variations of σ_1 of specimens with the distance from notch root, $r = 3$ (a) and 6 mm (b) (color online).

It can be seen from Fig. 6a that the maximum principal stress with notch radius of 3 mm increases first and then decreases with the increase of the distance from the notch root under different loads, and reaches maximum at the distance around 2.3 mm from the notch root. As depicted in Fig. 6b, for the tensile specimens with notch radius of 6 mm, as the distance from the notch root increases, the maximum principal stress under different loads shows an increasing trend, and the maximum principal stress reaches maximum around the center of the narrowest surface of the notched tensile bar. Combined with Figs. 6a and 6b, we can find that the variation trends of the maximum principal stress of the two specimens with different notch radii are different, and the regions where the maximum principal stress reaches maximum are also distinguishing. The main reason for the local high stress state in discontinuous specimens is that the orientation of crystals compared to the direction of external loading is random. Actually, if the existence of macrodiscontinuity (such as notch) is the cause of the local high stress field in the specimen, the fracture volume of the material will be merely affected by the local high strength stress field namely the process zone [31]. This is probably the main reason why the calibration results of cleavage fracture parameters of two kinds of notch sizes are inconsistent. In order to further compare the difference between the distributions of the maximum principal stress of the two specimens, we select the same load of 94.2 kN, which is an intermediate value between the fracture loads of the two specimens. The distributions of the maximum principal stress under this load are plotted in Fig. 7.

Figure 7 shows that even under the same external load (F=94.2 kN), the variation trends of the maximum

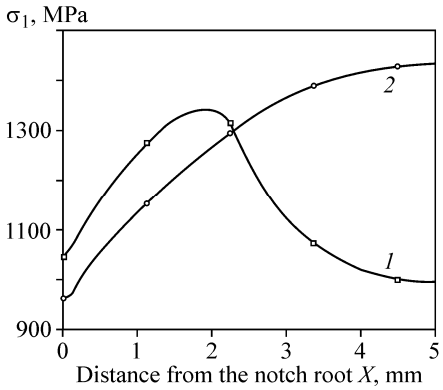

Fig. 7. Variations of σ_1 of the two specimens with the distance from the notch root, F = 94.2 kN, r = 3 (*1*) and 6 mm (*2*).

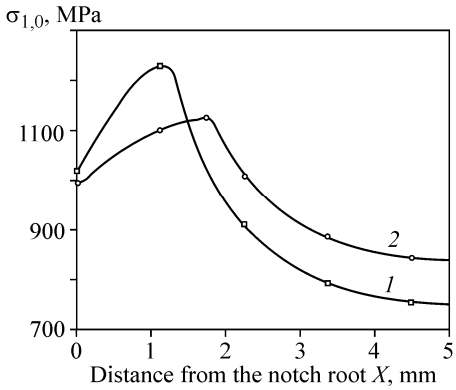

Fig. 8. Variations of $\sigma_{1,0}$ of the two specimens with the distance from the notch root, r = 3 (*1*) and 6 mm (*2*).

principal stress of the specimen with notch radius of 3 mm and the specimen with notch radius of 6 mm differ. Besides, the locations where the maximum principal stress reaches maximum in the two specimens are also different. That is, the areas where the fracture occurs in the two specimens are different. Moreover, the maximum value of the maximum principal stress of the specimen with notch radius of 3 mm is less than that of the specimen with notch radius of 6 mm, which indicates that the specimen with notch radius of 6 mm is more inclined to fracture than that with notch radius of 3 mm. This is consistent with the experimental results in Ref. [28].

In addition, Qian et al. [27] have claimed that the decisive factor that the new local approach model can overcome the ambiguity of parameters calibration of Beremin model is the introduction of $\sigma_{1,0}$. For this reason, we investigate the distributions of $\sigma_{1,0}$ of the above two kinds of specimens. Figure 8 shows the variations of $\sigma_{1,0}$ with the distance from the notch root in the above mentioned specimens.

As can be seen from Fig. 8, in the case of the same temperature, material and external loading, the regions where $\sigma_{1,0}$ reaches maximum in the two notched specimens are different. Meanwhile, the maximum value of $\sigma_{1,0}$ of the specimen with notch radius of 3 mm is greater than that of the specimen with notch radius of 6 mm. In other words, $\sigma_{1,0}$ also differs greatly with the notch size changing.

In summary, the effect of notch radius on Weibull parameters may be mainly due to the different stress concentration of specimens with different notch radii, and the different distributions of σ_1 and $\sigma_{1,0}$.

Considering σ_1 and $\sigma_{1,0}$ are the most important influencing factors when calculating Weibull stress in the new local approach model, their values will directly affect the results of Weibull stress. Then it will further influence the calibration results of Weibull parameters.

5. CONCLUSIONS

By using 3D finite element analysis and the new local approach model, the Weibull parameters of two different sized round notched bar tensile specimens of A508-C steel at –196°C have been calibrated. The calibration results of the specimens with notch radius of 3 mm are m = 11.888 and σ_0 = 984.360 MPa. As for the specimen with notch radius of 6 mm, the results shows that m = 25.833 and σ_0 = 664.255 MPa.

For the round notched bar tensile specimens with a fixed material, the calibration results of Weibull parameters are different when the notch size is different. That is to say, the calibration results of Weibull parameters of the new model are affected by the geometric size of the specimen.

The variation of Weibull parameters of the new model with the geometric size of the specimen is mainly due to the different stress concentration factors of specimens with different notch sizes, the different distribution trends of the maximum principal stress, and the different distributions of $\sigma_{1,0}$ introduced by the new model.

In this paper, we employ the experimental data of two sets of round notched bar tensile specimens with different notch radii and finite element analysis to approve the size-dependence of parameters calibration of the new local approach model. Note that the present work is just a preliminary study on the issue of size-dependence of calibrated parameters. The underlying microscopic mechanism concerning the issue remains unclear. So more sufficient experimental and numerical data and theoretical analysis are required to support the obtained conclusions in this study. Note that

the present work is only based on the data of A508-C steel under tensile conditions, the other types of ferritic steels and loading conditions shall be considered in the future work. Meanwhile, the present study indicates that probably the new local approach model also needs to be improved with respect to the determination of $\sigma_{1,0}$.

FUNDING

This work is funded by the Natural Science Foundation of Shanghai (Grant No. 19ZR1421400), the National Natural Science Foundation of China (Grants Nos. 11872364, 11932020), and the CAS Pioneer Hundred Talents Program.

REFERENCES

1. Qian, G., Lei, W.S., Peng, L., Yu, Z., and Niffenegger, M., Statistical Assessment of Notch Toughness Against Cleavage Fracture of Ferritic Steels, *Fatigue Fract. Eng. Mater. Struct*., 2017, vol. 41, no. 7, pp. 1–12.
2. Chen, J. and Cao, R., Micromechanism of Cleavage Fracture of Weld Metals, *Acta Metall. Sin*., 2017, vol. 53, no. 11, pp. 1427–1444.
3. Qian, G., Niffenegger, M., Sharabi, M., and Lafferty, N., Effect of Non-Uniform Reactor Cooling on Fracture and Constraint of a Reactor Pressure Vessel, *Fatigue Fract. Eng. Mater. Struct*., 2018, vol. 41, pp. 1559–1575.
4. Filho, W.W.B., Carvalho, A.L.M., and Bowen, P., Micromechanisms of Cleavage Fracture Initiation from Inclusions in Ferritin Welds. Part I. Quantification of Local Fracture Behavior Observed in Notched Testpieces, *Mater. Sci. Eng. A*, 2007, vol. 460–461, pp. 436–452.
5. Filho, W.W.B., Carvalho, A.L.M., and Bowen, P., Micromechanisms of Cleavage Fracture Initiation from Inclusions in Ferritin Welds. Part II. Quantification of Local Fracture Behavior Observed in Fatigue Pre-Cracked Testpieces, *Mater. Sci. Eng. A*, 2007, vol. 452–453, pp. 401–410.
6. Wang, G.Z., Liu, Y.G., and Chen, J.H., Investigation of Cleavage Fracture Initiation in Notched Specimens of a C–Mn Steel with Carbides and Inclusions, *Mater. Sci. Eng. A*, 2004, vol. 369, pp. 181–191.
7. He, J., Lian, J., Golisch, G., He, A., Di, Y., and Munstermann, S., Investigation on Micromechanism and Stress State Effects on Cleavage Fracture of Ferritic-Pearlitic Steel at –196°C, *Mater. Sci. Eng. A*, 2017, vol. 686, pp. 134–141.
8. Scibetta, M., A Cleavage Fracture Framework: New Perspectives in Cleavage Modeling of Ferritin Steels, *Eng. Fract. Mech*., 2016, vol. 160, pp. 147–169.
9. Pineau, A., Benzerga, A.A., and Pardoen, T., Failure of Metals I: Brittle and Ductile Fracture, *Acta Mater*., 2016, vol. 107, pp. 424–483.
10. Qian, G., Cao, Y., Niffenegger, M., Chao, Y.J., and Wu, W., Comparison of Constraint Analyses with Global and Local Approaches under Uniaxial and Biaxial Loadings, *Eur. J. Mech. A. Solids*, 2018, vol. 69, pp. 135–146.
11. Zhang, G.S., Jing, H.Y., Ma, C., Zhang, Y.F., and Huo, L.X., Advancement on the Brittle Fracture Assessment of Welded Joints Based on Local Approach, *Press. Vess. Technol*., 2003, vol. 20, no. 7, pp. 43–47.
12. Beremin, F.M., Pineau, A., Mudry, F., Devaux, J.C., D'Escatha, Y., and Ledermann, P., A Local Criterion for Cleavage Fracture of a Nuclear Pressure Vessel Steel, *Metall. Mater. Trans. A*, 1983, vol. 14, no. 11, pp. 2277–2287.
13. Pineau, A., Development of the Local Approach to Fracture over the Past 25 Years: Theory and Applications, *Int. J. Fracture*, 2006, vol. 138, no. 1–4, pp. 139–166.
14. Shen, A.R., Li, P.C., Wang, K.Y., Qian, G., and Berto, F., A Simplified Method for Parameters Calibration of the New Local Approach Model for Cleavage Fracture in a Ferritic Steel, *Theor. Appl. Fract. Mech*., 2019, vol. 100, pp. 426–433.
15. Qian, G., Gonzalez-Albuixech, V.F., and Niffenegger, M., Calibration of Beremin Model with the Master Curve, *Eng. Fract. Mech*., 2015, vol. 136, pp. 15–25.
16. Minami, F., Estimation Procedure for the Weibull Parameters Used in the Local Approach, *Int. J. Fracture*, 1992, vol. 54, no. 3, pp. 197–210.
17. *ESIS P6-98. Procedure to Measure and Calculate Materials Parameters for the Local Approach to Fracture Using Notch Tensile Specimens*, ESIS Publication, 1998. Available at http://www.lavoisier.eu/books/other/esis-procedure-p6-98-procedure-to-measure-et-calculatematerial-parameters-for-the-local-approach-to-fracture-usingnotched-tensile-specimens/description_22722-90
18. Akbarzadeh, P. and Hadidimoud, S., On Geometry Dependence of Weibull Parameters; Beremin Approach Revisited, *14th Annual International Mechanical Engineering Conference*, May 2006, Isfahan University of Technology, Isfahan, Iran.
19. Cao, Y., Hui, H., Wang, G., and Xuan, F.Z., Inferring the Temperature Dependence of Beremin Cleavage Model Parameters from the Master Curve, *Nucl. Eng. Des*., 2011, vol. 241, no. 1, pp. 39–45.
20. Hadidi-Moud, S., Mirzaee-Sisan, A., Truman, A., and Smith, D.J., A Local Approach to Cleavage Fracture in Ferritic Steels Following Warm Pre-Stressing, *Fatigue Fract. Eng. Mater. Struct*., 2010, vol. 27, no. 10, pp. 931–942.
21. Gao, X., Zhang, G., and Srivatsan, T.S., Prediction of Cleavage Fracture in Ferritic Steels: A Modified Wei-

bull Stress Model, *Mater. Sci. Eng. A*, 2005, vol. 394, no. 1, pp. 210–219.
22. Petti, J.P. and Dodds, R.H., Calibration of the Weibull Stress Scale Parameter, Using the Master Curve, *Eng. Fract. Mech*., 2005, vol. 72, no. 1, pp. 91–120.
23. Lei, W.S., A Cumulative Failure Probability Model for Cleavage Fracture in Ferritic Steels, *Mech. Mater*., 2016, vol. 93, pp. 184–198.
24. Lei, W.S., A Framework for Statistical Modelling of Plastic Yielding Initiated Cleavage Fracture of Structural Steels, *Philos. Mag*., 2016, vol. 96, pp. 3586–3631.
25. Qian, G., Lei, W.S., Niffenegger, M., and Gonzalezalbuixech, V.F., On the Temperature Independence of Statistical Model Parameters for Cleavage Fracture in Ferritic Steels, *Philos. Mag*., 2018, vol. 98, pp. 959–1004.
26. Hui, H. and Li, P.N., Study on Fracture of Notch Bars at Low Temperature with Local Approach, *J. Mech. Eng*., 2009, vol. 45, no. 10, pp. 306–312 (in Chinese).
27. Qian, G., Lei, W.S., and Niffenegger, M., Calibration of a New Local Approach to Cleavage Fracture of Ferritic Steels, *Mater. Sci. Eng. A*, 2017, vol. 694, pp. 10–12.
28. Hui, H., *Study on Key Technology Improvement and Application of Local Approach for Cleavage Fracture*: Ph.D. Dissertation, East China University of Science and Technology, 2002 (in Chinese).
29. Chakraborti, P.C., Kundu, A., and Dutta, B.K., Weibull Analysis of Low Temperature Fracture Stress Data of 20MnMoNi55 and SA333 (Grade 6) Steels, *Mater. Sci. Eng. A*, 2014, vol. 594, pp. 89–97.
30. Zhang, S.M., *Practical Stress Concentration Manual*, Shaanxi: Shaanxi Science and Technology Press, 1984 (in Chinese).
31. Milella, P.P. and Bonora, N., On the Dependence of the Weibull Exponent on Geometry and Loading Conditions and Its Implications on the Fracture Toughness Probability Curve Using a Local Approach Criterion, *Int. J. Fracture*, 2000, vol. 104, no. 1, pp. 71–87.